J Mater Sci: Mater Med (2012) 23:1033–1044
DOI 10.1007/s10856-012-4556-z

Application of K/Sr co-doped calcium polyphosphate bioceramic as scaffolds for bone substitutes

Huixu Xie · Qianbin Wang · Qingsong Ye · Changxiu Wan · Longjiang Li

Received: 9 October 2011 / Accepted: 11 January 2012 / Published online: 5 February 2012

Abstract Ion doping is one of the most important methods to modify the properties of bioceramics for better biodegrade abilities, biomechanical properties, and biocompatibilities. This paper presents a novel ion doping method applied in calcium polyphosphate (CPP)-based bioceramic scaffolds substituted by potassium and strontium ions (K/Sr) to form (K/Sr–CPP) scaffolds for bone tissue regeneration. The microstructure and crystallization of the scaffolds were detected by scanning electron microscopy and X-ray diffraction. Compressive strength and degradation tests were assessed to evaluate the mechanical and chemical stabilities of K/Sr–CPP in vitro. The cell biocompatibility was measured with respect to the cytotoxicity of the extractions of scaffolds. Muscle pouches and bone implantation were performed to evaluate the biodegradability and osteoconductivity of the scaffolds. The results indicated that the obtained K/Sr–CPP scaffolds had a single beta-CPP phase. The unit cell volume and average grain size increased but the crystallization decreased after the ions were doped into the CPP structure. The K/Sr–CPP scaffolds yielded a higher compressive strength and a better degradation property than the pure CPP scaffold. The MTT assay and in vivo results reveal that the K/Sr–CPP scaffolds exhibited a better cell biocompatibility and a tissue biocompatibility than CPP and hydroxyapatite scaffolds. This study proves the potential applications of K/Sr–CPP scaffolds in bone repair.

1 Introduction

Developing controllably biodegradable materials as bone graft substitutes for filling large bone defects remains a main task in biomaterials research. In general, an ideally degradable biomaterial can controllably degrade to match the rate of new tissue regeneration. Calcium polyphosphate (CPP), a novel bioceramic as a bone substitute, has been rapidly developed since it was invented 10 years ago [1–4]. CPP has drawn attentions because of its outstanding biocompatibility [5, 6], controllable degradability [7], excellent mechanical property, and compositional similarities to natural bone [8, 9]. Grynpas found that the CPP scaffold supported bone in growth without an adverse reaction after it was implanted in the distal femur of rabbits [2]. This result suggests that the CPP scaffold had its potential as a bone implant material. Many in vivo experiments also indicate that the CPP scaffolds showed excellent osteoconductivities and can be used as an ideal bone substitute material [2–4].

Huixu Xie and Qianbin Wang contributed equally to this work.

H. Xie · Q. Ye · L. Li (✉)
State Key Laboratory of Oral Diseases, West China Hospital of Stomatology, Sichuan University, Chengdu 610061, People's Republic of China
e-mail: muzili63@163.com

Q. Wang
School of Chemistry and Environment, Beihang University, Beijing 100191, People's Republic of China

Q. Ye
Department of Orthodontics, School of Medicine and Dentistry, James Cook University, Cairns, QLD 4878, Australia

C. Wan
Department of Polymer Science and Engineering, Sichuan University, Chengdu 610065, People's Republic of China

The degradability of CPP was found to be low, which suggests that the CPP scaffolds might not match bone growth rates when they are implanted in bone structures. Aimed at improving its degradability, Song studied the effect of ion doping in CPP on its degradability and mineralization [10]. The results indicate that the doped elements significantly affected the properties of CPP. Wang [11] also proved that alkali metal and strontium ions can be co-substituted in CPP. In particular, the co-ion implantation had improved degradability and mineralization of CPP when a saline solution was used as the degradation medium.

However, little is known with respect to the influence of co-doped CPP structures on their microstructures, mechanical properties, and biocompatibilities. In this paper, we further studied potassium and strontium co-substituted CPP scaffolds regarding their biodegradability, biomechanical property and biocompatibility. To mimic the body conditions, we used simulated body fluid (SBF) to characterize the effects of K/Sr co-doped CPP on the degradation behavior in vitro. The mechanical properties of K/Sr–CPP scaffolds were examined in terms of compressive strength. Proliferation of human osteoblast-like cells was used to evaluate the cell biocompatibility of K/Sr–CPP in vitro. In vivo biodegradability, biocompatibility and osteogenesis property of K/Sr–CPP scaffolds were investigated to use a rabbit model to demonstrate their potential applications as bone substitutes.

2 Materials and methods

2.1 Preparation of porous CPP, K/Sr–CPP and hydroxyapatite (HA) scaffolds

K/Sr co-substituted β-CPP powders were synthesized by gravity sintering. The $CaCO_3$ powder containing the total amount of Ca^{2+} ion was mixed with 4 mol% K_2CO_3 and 2 mol% $SrCO_3$ to prepare K/Sr–CPP with a molar ratio of Ca/K/Sr = 90/8/2. The mixture was added slowly into the 85% phosphoric acid and stirred to prepare $Ca_{0.9}K_{0.08}Sr_{0.02}(H_2PO_4)_2 \cdot H_2O$ based on the following reaction:

$$0.9CaCO_3 + 0.04K_2CO_3 + 0.02SrCO_3 + 2H_3PO_4 \rightarrow Ca_{0.9}K_{0.08}Sr_{0.02}(H_2PO_4)_2 \cdot H_2O + CO_2 \quad (1)$$

After the reaction continued at room temperature overnight, the solution was evaporated in vacuum. The precipitates washed by 95% ethanol and then collected by filter paper until the pH of the filter paper reached about 7. These precipitates were sintered at 500°C for 10 h, then heated to 1,200°C for 1 h to form amorphous K/Sr–CPP glass according to the following reactions:

$$Ca_{0.9}K_{0.08}Sr_{0.02}(H_2PO_4)_2 \cdot H_2O \rightarrow Ca_{0.9}K_{0.08}Sr_{0.02}(H_2PO_4)_2 + H_2O \quad (2)$$

$$Ca_{0.9}K_{0.08}Sr_{0.02}(H_2PO_4)_2 \rightarrow Ca_{0.9}K_{0.08}Sr_{0.02}H_2P_2O_7 + H_2O \quad (3)$$

$$n\ Ca_{0.9}K_{0.08}Sr_{0.02}H_2P_2O_7 \rightarrow n\ Ca_{0.9}K_{0.08}Sr_{0.02}(PO_3)_2 + n\ H_2O \quad (4)$$

After crushing the amorphous K/Sr–CPP glass by an agate motor, the powders with a size range smaller than 75 μm was mixed with stearic acid to fabricate porous K/Sr–CPP scaffolds as described earlier [12]. Pure β-CPP scaffolds were prepared using the same method. Porous HA scaffolds were also studied for comparison, which were provided by Engineering Research Center in Biomaterials, Sichuan University.

2.2 Microstructure characterization

Powder X-ray diffraction (XRD) analysis was performed to identify crystalline phases and lattice constants of the K/Sr–CPP and CPP powders using an X-ray diffractometer (X'Pert Pro MPD, Philips, Netherlands). CoKα was applied at 40 kV and 40 mA. The crystal lattice parameters and crystallinity were calculated according to the XRD patterns by software JADE 5.0 installed in the diffractometer.

The microstructures of the K/Sr–CPP and CPP scaffolds were examined by a scanning electron microscope (SEM) (Hitachi S2400). Average grain sizes of the two scaffolds were determined by the linear intercept method [13].

2.3 In vitro degradation test

The in vitro degradation test for the K/Sr–CPP and CPP scaffolds was performed in SBF [10] for 28 days at 37 ± 0.5°C. The quantitative determination of ions released into the SBF was measured to characterize the degradability of the K/Sr–CPP and CPP scaffolds degraded for 1, 3, 5, 8, 13, 18, 23 and 28 days, respectively. The phospho–vanado–molybdate method [14] and calcein titration method [15] were used to measure the concentrations of PO_4^{3-} and Ca^{2+} released in the degradation solution, respectively.

2.4 Mechanical assessment

A universal materials testing machine (Instron 4302, USA) was used to measure the compressive strength of the K/Sr–CPP and CPP scaffolds. The cylindrical samples were prepared with a diameter of 10 mm and a length of 10 mm after they were immersed in the SBF at 37°C for 0, 14 and

28 days, respectively, and dried at 80°C for 24 h. The loads were applied at the loading rate of 1 mm/min to fracture the samples. Five repeats for each material were conducted to obtain the mean strength values and the standard deviations.

2.5 MTT assay

Human osteoblast-like cells (MG63) was selected in this study, which were made by the State Key Laboratory of Oral Diseases, Sichuan University. These cells were cultured in 25-cm^2 tissue culture flasks at 37°C with 5% fully humidified CO_2 in RPMI (Roswell Park Cancer Institute) 1640 medium (Invitrogen Corporation, USA). RPMI 1640 had a PH value of 7.4 and contained supplemented 10% fetal bovine serum (FBS) and 1% penicillin/streptomycin. It was changed every two days.

Cell proliferation was analyzed to evaluate the cytotoxicity of the K/Sr–CPP, CPP and HA scaffolds by MTT (3-[4, 5-dimethylthiazol-2-yl]-2, 5-diphenyltetrazolium bromide). HA scaffolds served as the control samples, which have been used as biomaterials in clinical applications. Scaffold samples with dimensions of 10-mm diameter and 1-mm length were extracted at 37°C for 24 h in saline solution at a ratio 0.75 cm^2/mL of the scaffold samples to the volume of saline solution [16]. Briefly, 4×10^3 cells per well were seeded in a 96-well microplate (Corning) with the final volume being 100 μL. After an overnight incubation, the cells were then cultured with a mixture of medium and degradation fluid. The extracts of K/Sr–CPP, CPP and HA scaffolds were added into each well ($n = 5$). One plate was taken out on the second, fourth and sixth days, respectively. The 20 μL/well MTT solution mixed with 5 mg/mL phosphate buffered saline (PBS) were added into the plate. The plate was incubated at 37°C for another 4 h. After that, MTT solution was removed and replaced by 150 μL DMSO, and the plates were shaken for 10 min. The optical density (OD) of each well was measured by a Microplate Reader (Model550, Bio Rad Corporation) at the wavelength of 490 nm to evaluate the cell numbers which were proportional to the OD value.

2.6 In vivo implantation

All procedures performed on animals were approved by Animal Ethics committee at Sichuan University. Twenty-seven healthy New Zealand white rabbits weighting about 2.5 ± 0.4 kg each were anesthetized with pentobarbital sodium. For each rabbit, a parallel lengthwise incision was made on the back of the rabbit after a piece of skin was prepped and sterilized with iodine. Then, the unilateral muscle of the spinal column was exposed and an incision was cut on the muscle to make a small pouch where a scaffold was implanted. After the implantation, the wound was closed. For bone implantation, a defect approximately 15 × 5 mm above the thighbone was filled with the prepared scaffold with dimensions of 15 mm × 5 mm × 4 mm. Each group rabbits were sacrificed after implantation for 4, 8 and 12 weeks. The scaffolds with surrounding tissue were excised, fixed in 10% neutral buffered formalin, decalcified and embedded in paraffin. The embedded tissue blocks were sectioned and stained with hematoxylin and eosin (H&E), and the histological sections were observed using a light microscope (BX41, Olympus, Japan).

2.7 Image analysis

The quantification of inflammatory cells was performed by counting the number of positive cells in micrographs (× 400) taken in six areas equally distributed in the scaffold of each disk. Disks from four different animals ($n = 3$) of each time point were used to calculate the mean values. All analyses and determinations were repeated at least three times by two independent investigators on blinded samples.

Quantitative determinations of newly formed bone and residual material were performed using image and statistical analysis of histological sections. In every implantation time, six pieces of histological sections were randomly chosen from K/Sr–CPP, HA and CPP groups. After stained with H&E, each section was observed under a light microscope at 50× magnification and at 10 different locations selected randomly. All analyses and determinations were repeated at least three times by two independent investigators on blinded samples. Using image analytical software Image-ProPlus (Media Cybernetics, USA), new bone volume (NBV) was expressed as the percentage of newly formed bone area in the available pore space (bone area/pore area × 100%).

2.8 Statistical analysis

Statistical analysis was performed by software SPSS12.0 (SPSS, Inc., Chicago, IL).The experimental data obtained in this paper were presented as means ± standard deviation (SD). Differences between groups were determined by one-way ANOVA, with a significance level of $p < 0.05$.

3 Results

3.1 XRD analysis

Figure 1 was the XRD pattern of CPP and K/Sr–CPP obtained in this study. It can be seen from the XRD pattern

of K/Sr–CPP (Fig. 1a) that the obtained sample consisted of a single beta-CPP phase, which is confirmed from observed characteristic peaks at diffracted angles (2θ) 27.878°, 29.516° and 33.161°, respectively, for crystal plane (014), (022) and (122) (PDF 77–1953). In addition, the XRD patterns show no significant difference in crystallized phase between the CPP and K/Sr–CPP, which indicated that the foreign metallic ions (8 mol% K^+ and 2 mol% Sr^{2+}) did not affect the crystallized phase of CPP structure.

The crystal lattice parameters of CPP and K/Sr–CPP are shown in insert of Fig. 1. The unit cell volume, a–, b– and c–axis unit cell parameters of K/Sr–CPP shown a slight increase compared with pure CPP. Potassium and strontium ions replace calcium ions in the CPP crystal lattice and affect the unit parameters of CPP due to the difference of substituted ionic radii. The ionic radii of K^+, Sr^{2+} and Ca^{2+} have been reported to be 0.133, 0.113 and 0.100 nm, respectively. The ionic radius of Sr^{2+} and K^+ ion is larger than that of Ca^{2+} ion, which led to the increasing of the unit cell volume.

Ion doping is one of most important methods to modify the bioceramics. The doped cationic, such as K^+, Na^+, Mg^{2+}, Zn^{2+} and Sr^{2+} substitutes Ca^{2+} site in the CPP crystal lattice. All of these cationic ions can introduce some specific changes into the CPP crystal. As previous study by Song [10], the incorporation of K^+ into the CPP structure changed the lattice parameters and its degradability and mineralization. And the substitution of Sr^{2+} for Ca^{2+} results in a slight increase in the unit cell parameters but an obvious decrease in degradability. Based on previous study, we prepared a novel CPP based bioceramic doped by K^+ and Sr^{2+} to improve the degradability and biocompatibility of CPP in this work. From the XRD pattern shown in Fig. 1, it is observed that some lattice parameters were changed, which may affect the properties of CPP.

3.2 Microstructure analysis

The effect of ions doped on the surface morphologies of CPP were presented in Fig. 2a and b. From the SEM micrographs, it can be seen that obvious amorphous area existed in K/Sr–CPP (Fig. 2a identified by blank arrow), while the surface morphology of CPP was more density and smooth. In order to qualitative analysis the effect of K^+ and Sr^{2+} doped on the average grain size of CPP, lineal intercept method was used to measure the value of grain size of samples, which was shown in Fig. 2c. After doped by K/Sr ions, the average grain size of CPP was increased from (3.48 ± 0.78) μm for pure CPP to (4.51 ± 0.78) μm. The crystallization of samples fit by software JADE 5.0 were presented in Fig. 2d. The incoming foreign ions, K^+ and Sr^{2+}, could reduce the crystallization of CPP samples from (86.74 ± 4.46)% for pure CPP to (70.32 ± 4.98)%,

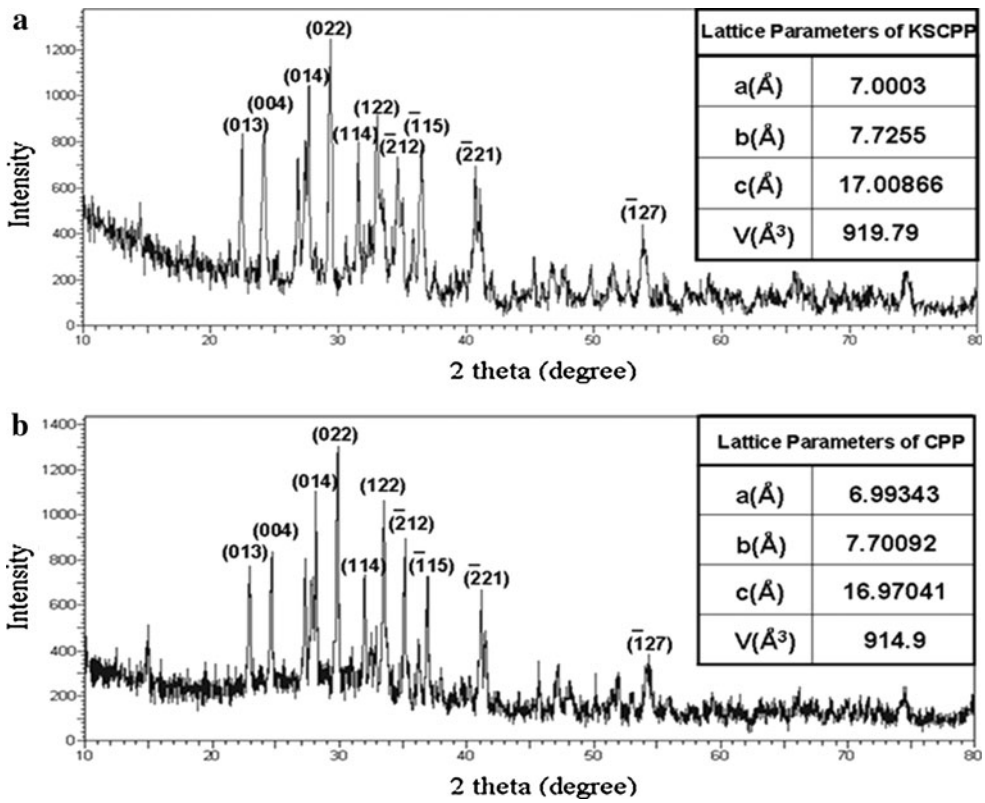

Fig. 1 XRD patterns and crystal lattice parameters of (**a**) K/Sr–CPP and (**b**) CPP

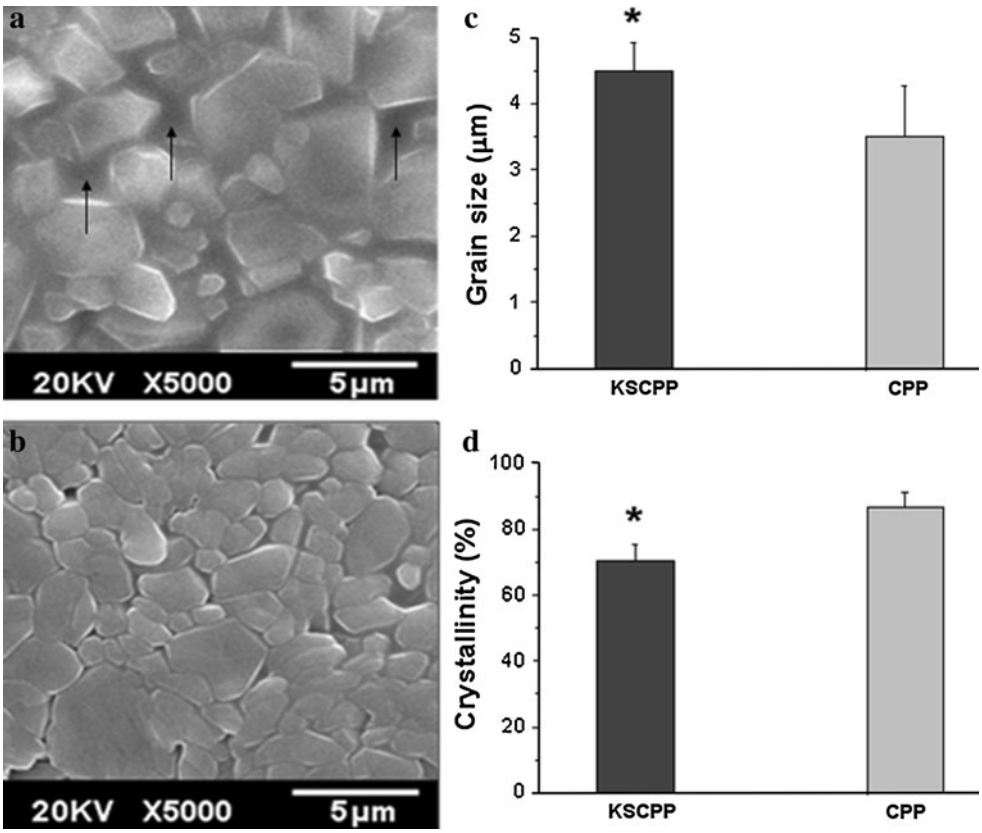

Fig. 2 The scanning electron micrographs of (**a**) K/Sr–CPP scaffold, (**b**) CPP scaffold, (**c**) average grain sizes of K/Sr–CPP and CPP scaffolds, and (**d**) crystallization of K/Sr–CPP and CPP scaffolds

which was accordance with the amorphous area observed by SEM (Fig. 2a identified by blank arrow).

3.3 Degradation in SBF

The release rates of Ca^{2+} and PO_4^{3-} of CPP and K/Sr–CPP scaffolds are presented in Fig. 3. Both the two patterns of scaffolds exhibited an incessant increase of the Ca^{2+} and PO_4^{3-} concentrations in SBF with degradation time. But compared with CPP, the K/Sr–CPP scaffold exhibited a higher degradation rate at each time points. It can be seen that the PO_4^{3-} and Ca^{2+} concentrations released into SBF of K/Sr–CPP scaffold are considerably larger than that of CPP scaffold (920 mg/L $>$ 312 mg/L, 204 mg/L $>$ 61 mg/L) after degradation for 28 days.

As proved by Pilliar [1], the amorphous and grain boundary regions, contained many disorder atoms or molecules, were the weakness points in CPP crystal. And the degradation media could attack these areas easily, which led to a rapid degradation in the initial period of immersion. From the SEM micrographs shown in Fig. 2a and 2b, it can be clearly observed that the crystal grains of CPP were more intimately connected with each other, while K/Sr–CPP exhibited a larger area of grain boundary and amorphous regions, indicating that the K/Sr–CPP could be more easily attacked by SBF. As a consequence, the degradation rate of K/Sr–CPP scaffold was higher than that of CPP scaffold.

Degradability is one of important properties of bone implant materials because it is crucial for bone induction, conduction, metabolism and longevity when implanted into body. In general, materials should be controllable degradation to match the rate of new tissue regeneration. For CPP, the degradation behavior in vitro may be the result of physical abrasion and chemical dissolution. Firstly, the physical factors, such as porosity, crystallinity and grain size, could affect the abrasion, fracture and disintegration process when CPP was immersion in degradation media. Secondly, chemical factor included on composition and ionic substitutions in materials play an important role in the degradation behavior of CPP in vitro. In previous study, our group had focused on the physical and chemical degradation of CPP and found the crystal structure [17], sintering time and temperature [11], polymerization degree [7], ion doped [10] and degradation media [18] can control its degradation process (Fig. 3c).

3.4 The effect of ions doped on the degradability of CPP

It had been reported [19] that the doped ion's radius and electrical charge played a dominant role in the degree of

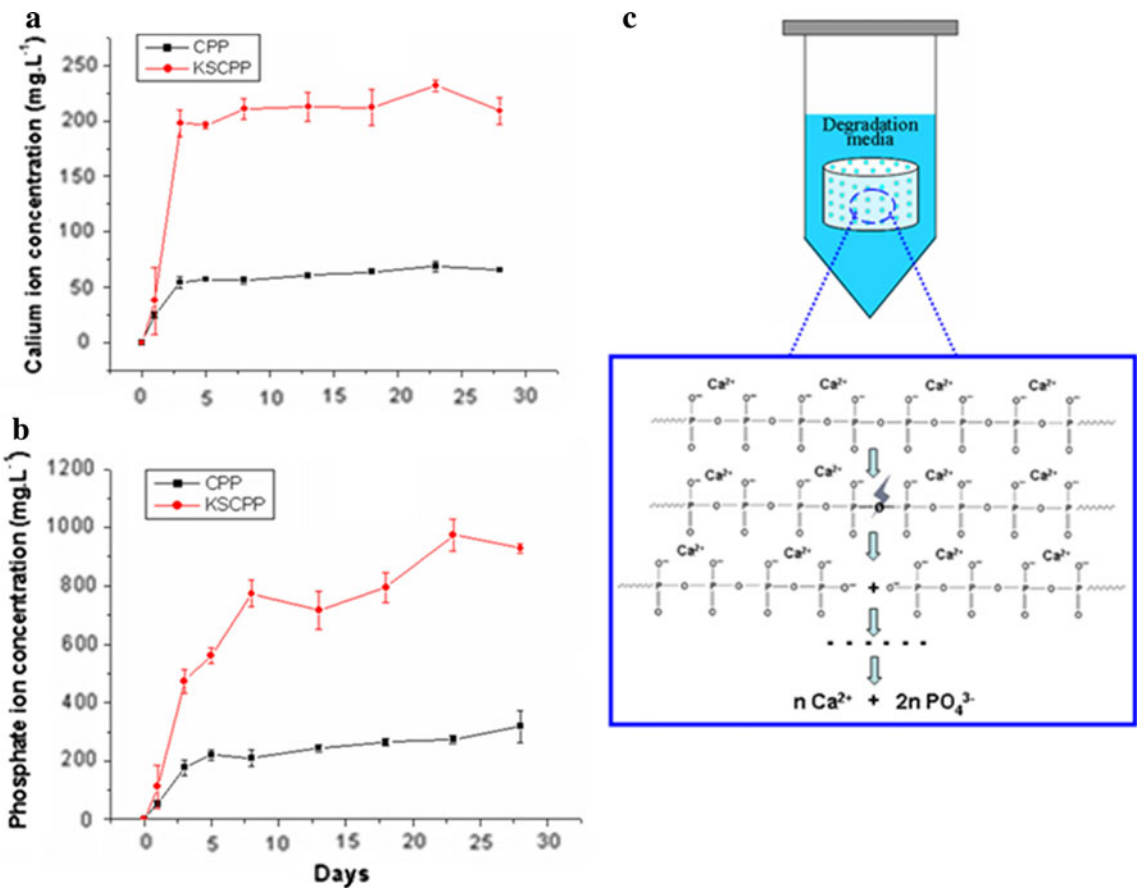

Fig. 3 Ca^{2+} ion concentration (**a**), PO_4^{3-} ion concentration (**b**) concentrations in SBF and the degradation mechanism of CPP (**c**)

point defects, which can significantly affect the properties of ceramic. Figure 4 presented the potential mechanism of ions doping in CPP crystal lattice. A possible defect reaction for the incorporation of $Sr(PO_3)_2$ into the $Ca(PO_3)_2$ lattice is

$$SrM_2 \xrightarrow{CaM_2} Sr_{Ca} + 2M_M(M = PO_3^-) \quad (5)$$

According to this equation, the effect of $Sr(PO_3)_2$ would not be to increase the defect of CPP. In addition, calcium and strontium are in the same group on the periodic table and the radius of Ca^{2+} and Sr^{2+} are 0.100 nm $(r_{Ca^{2+}})$ and 0.113 nm $(r_{Sr^{2+}})$ respectively. Thus the radius ratio of $(r_{Sr^{2+}} - r_{Ca^{2+}})/r_{Ca^{2+}}$ is less than 15%. Besides, the electrovalence of both ions is +2. According to the Hume–Rothery Rules [20], the strontium ions could enter into the crystal lattices of CPP without breaking its initial crystal structure and an infinitely soluble solid solution was formed. Thus, the metallic ions with an approached ionic radius and electrical charge contribute to form a more chemical stable calcium polyphosphate. As previous study, strontium-doped CPP scaffold exhibited a lower degradation rate than CPP scaffold [21], which supports this theory.

For the incorporation of KPO_3 into the $Ca(PO_3)_2$ lattice, a possible defect reaction is

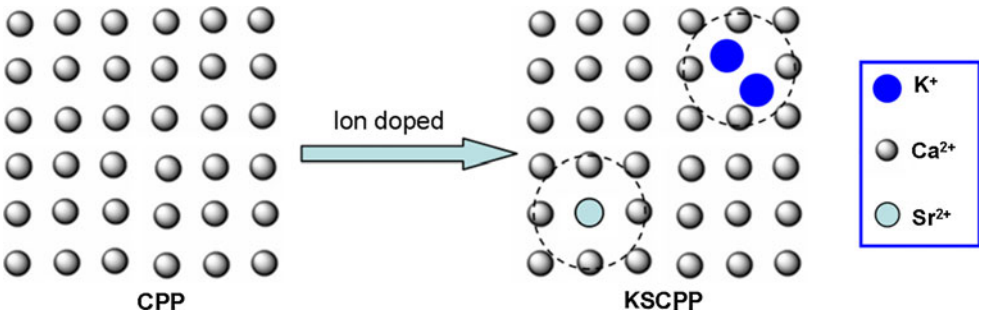

Fig. 4 The potential mechanism of ions doping in CPP crystal lattice

$$2KM \xrightarrow{CaM_2} K'_{Ca} + K^{\cdot} + 2M_M(M = PO_3^-) \quad (6)$$

According to this equation, the effect of KPO_3 would increase the concentration of potassium interstitial ions, which result in the instability of CPP bioceramics. Moreover, the radius of K^+ is 0.133 nm (r_{K^+}), indicating that the radius ratio of $(r_{K^+} - r_{Ca^{2+}})/r_{Ca^{2+}}$ is more than 15%. In addition, the groups on the periodic table and electrovalence of K^+ and Ca^{2+} are different. According to the Hume–Rothery Rules [20], the doped K ions created much point defects of CPP crystal, which reduced the stability of its crystal structure. Combine with the degradability shown in Fig. 3, it can be seen that the incorporation of K^+ cause imbalances in the charges to disorder the crystal structure of CPP, which result in the degradation promotion.

3.5 Mechanical properties of scaffolds

The mean compressive strength values of CPP and K/Sr–CPP scaffolds with 40% porosity aged in SBF for 0, 14 and 28 days were presented in Fig. 5. It was observed a significant difference between these two scaffolds. The initial compressive strength (before degradation, 0 day) was increased from (1.51 ± 0.47) MPa to (2.40 ± 0.27) MPa after doped with K/Sr ions. After degraded in SBF for 14 days, the compressive strength of K/Sr–CPP showed a sharp decreased to (0.75 ± 0.20) MPa. While for CPP, the compressive strength was no difference compared with the initial value. After immersion in SBF for 28 days, the compressive strength of scaffolds were both constantly decreased during immersion period. The compressive strength for K/Sr–CPP scaffolds decreased from (0.75 ± 0.20) MPa to (0.67 ± 0.15) MPa, while that of CPP scaffolds decreased from (1.48 ± 0.18) MPa to (0.76 ± 0.14) MPa from 14 days to 28 days. The sharp decreased of K/Sr–CPP may be resulted from the rapid degradation of CPP in SBF as shown in Fig. 3.

Biomechanics is one important function of bone. So the design of scaffold for bone tissue engineering must have reasonable mechanical strength. In general, the scaffold would provide a stable mechanical environment similar to the natural bone. Compared with the mechanical strength of cancellous bone (1–10 MPa) [19], it revealed that the porous CPP and K/Sr–CPP scaffold could meet the mechanical requirement, which meant the scaffold could support new bone tissue regeneration when implanted in body. However, the mechanical strength of K/Sr–CPP was not very good after degradation. For further investigating, we will pay attention to modify the bioceramic (e.g. organic/bioceramic composition) to reduce this rapid mechanical decreased.

3.6 In vitro cell proliferation

MTT assay is an important method to evaluate the cytotoxicity of the extractions of scaffolds. Figure 6 showed the cytotoxicity result of CPP and K/Sr–CPP with HA served as the control. The OD values revealed that the cell proliferation increased with the culture time on the three groups. However, it was clear that the growth rate was K/Sr–CPP > CPP > HA during the entire culture period, indicating that K/Sr–CPP was nontoxic. And, K/Sr–CPP exhibited a better biocompatibility in vitro than CPP and HA.

It had been proved that Sr^{2+} had the ability to enhance bone cell replication and bone formation in vitro [22, 23]. Qiu [23] had found that SCPP could promote the growth

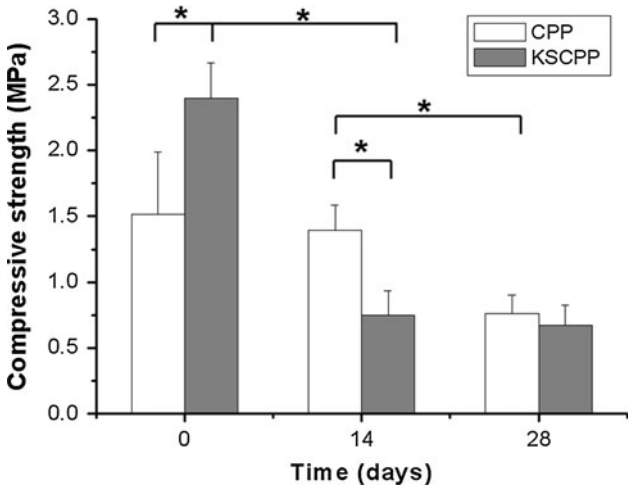

Fig. 5 Compressive strength of CPP and K/Sr–CPP scaffolds before and after degradation

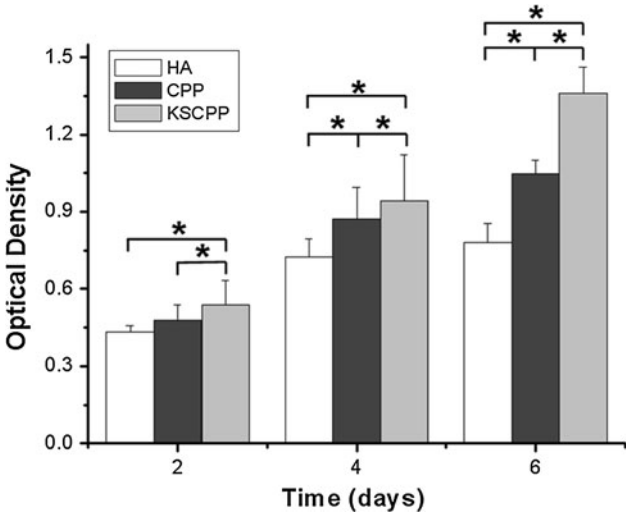

Fig. 6 MTT assay for proliferation of MG63 cultured in the extraction of CPP and K/Sr–CPP for different days

and adhesion of osteoblasts in vitro. In addition, slight K^+ had little side effect to human body and was often used as an ingredient of many medicines, for example, Penicillin V potassium. Considered together, the doped Sr and K ions improved the cell biocompatibility of K/Sr–CPP scaffold.

3.7 Intramuscular implantation

In muscle implantation experiment, all surgeries on the rabbits were completed successfully and the animals survived during the 12 postoperative weeks. Figure 7 showed the histological photographs of HA, CPP and K/Sr–CPP scaffolds after implantation in muscle pouches during the 12 weeks analysis period. Histological evaluation of the scaffolds–implanted tissues demonstrated differences in the response (Fig. 7). The K/Sr–CPP scaffolds–implanted tissues exhibited the typical structure of large fibrous tissues filled with vessels surrounded by a combination of implanted K/Sr–CPP scaffolds and muscle without the presence of new bone or a marrow cavity during the 12 weeks analysis period (Fig. 7c, f, i). In HA and CPP groups, both scaffolds degraded slower than K/Sr–CPP. The interface between materials and tissues was still clearly visible after implantation for 12 weeks (Fig. 7g, h).The CPP scaffolds–implanted produced much more variable results. In some cases, small amounts of new fibrous tissues formed in the scaffold (Fig. 7h). The interface between materials and tissues was still clearly visible after implantation for 12 weeks (Fig. 7g, h). Significantly more giant cells were formed around K/Sr–CPP scaffolds than HA and CPP from week 2 on (Fig. 7). Yet phagocytosis (as revealed by light microscopy) was never observed during the whole time course of the foreign body reaction (FBR) in either HA,CPP or K/Sr–CPP implants. It was clear that the degradation rate was K/Sr–CPP > CPP > HA during the entire period, indicating that K/Sr–CPP was nontoxic.

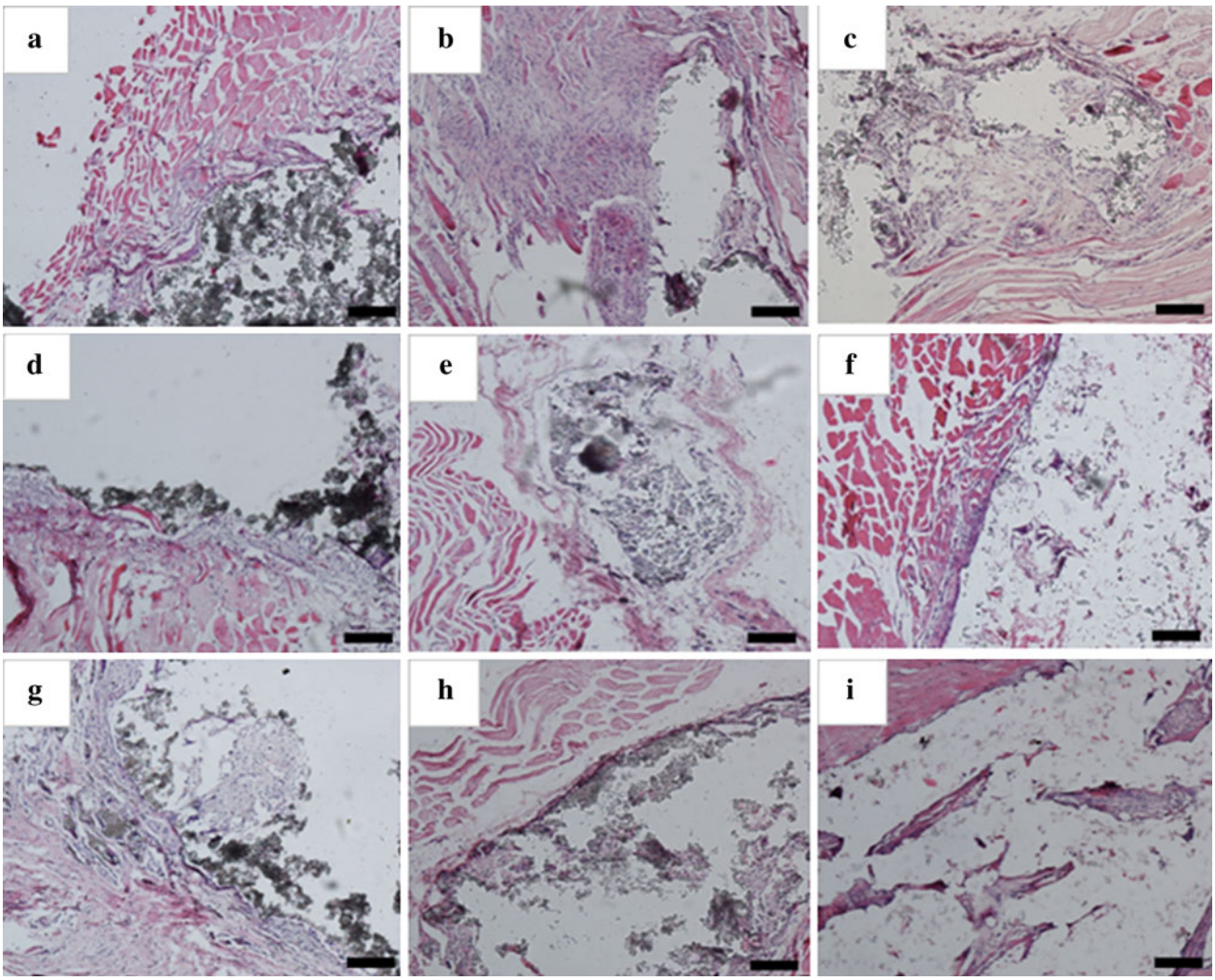

Fig. 7 Histological sections of HA, CPP and K/Sr–CPP scaffolds after 4(**a**, **b**, **c**), 8(**d**, **e**, **f**) and 12(**g**, **h**, **i**) weeks of muscle implantation (HA: **a**, **d**, **g**; CPP: **b**, **e**, **h**; K/Sr–CPP: **c**, **f**, **i**)

3.8 Bone implantation

In bone implantation experiment, all surgeries on the rabbits were completed successfully and the animals survived during the 12 postoperative weeks. None of the implanted sites of the rabbits showed any infection and inflammation after the operation. Figure 8 shows optical images of H&E histological staining of the HA, CPP and K/Sr–CPP scaffolds after implantation. Both tissue response and degradation surrounding the scaffold could be observed.

After 4 weeks of implantation, the interfaces of all the scaffolds were clearly visible. New bone was observed in the margins of the implant, the scaffolds became loosen and there was no new bone formation in the center of the K/Sr–CPP scaffolds (Fig. 8c1). HA scaffolds did not adhere to the bone closely, which there was not the direct evidence of bone formation (Fig. 8b1). New bone and bone lacuna was observed in the margins of the implant and degradation of the CPP scaffold was not observed (Fig. 8a1).With the implantation prolonged, more newly formed bone tissues, including bone trabecular and lacuna, were observed in the K/Sr–CPP group after implantation for 8 weeks (Fig. 8c2). Small area and sporadic new bone was in the center of the K/Sr–CPP scaffolds. In addition, degradation of the scaffold was observed, indicated by the loss of integrity of the implant and concomitant replacement by newly formed bone with increasing implantation time. In contrast, newly formed bone increased gradually and degradation was not observed in the HA scaffold (Fig. 8b2). In the CPP group, newly formed bone and lacuna increased gradually both in quantity and maturation, and CPP scaffolds became loosen (Fig. 8a2). Finally, after 12 weeks of implantation new bone regenerated and penetrated through the interconnective pores to the center of the scaffolds. In the case of the K/Sr–CPP group, the interface between material and host bone was hardly detectable and formed a close union without any gap, and the large new bone in the center of scaffolds with

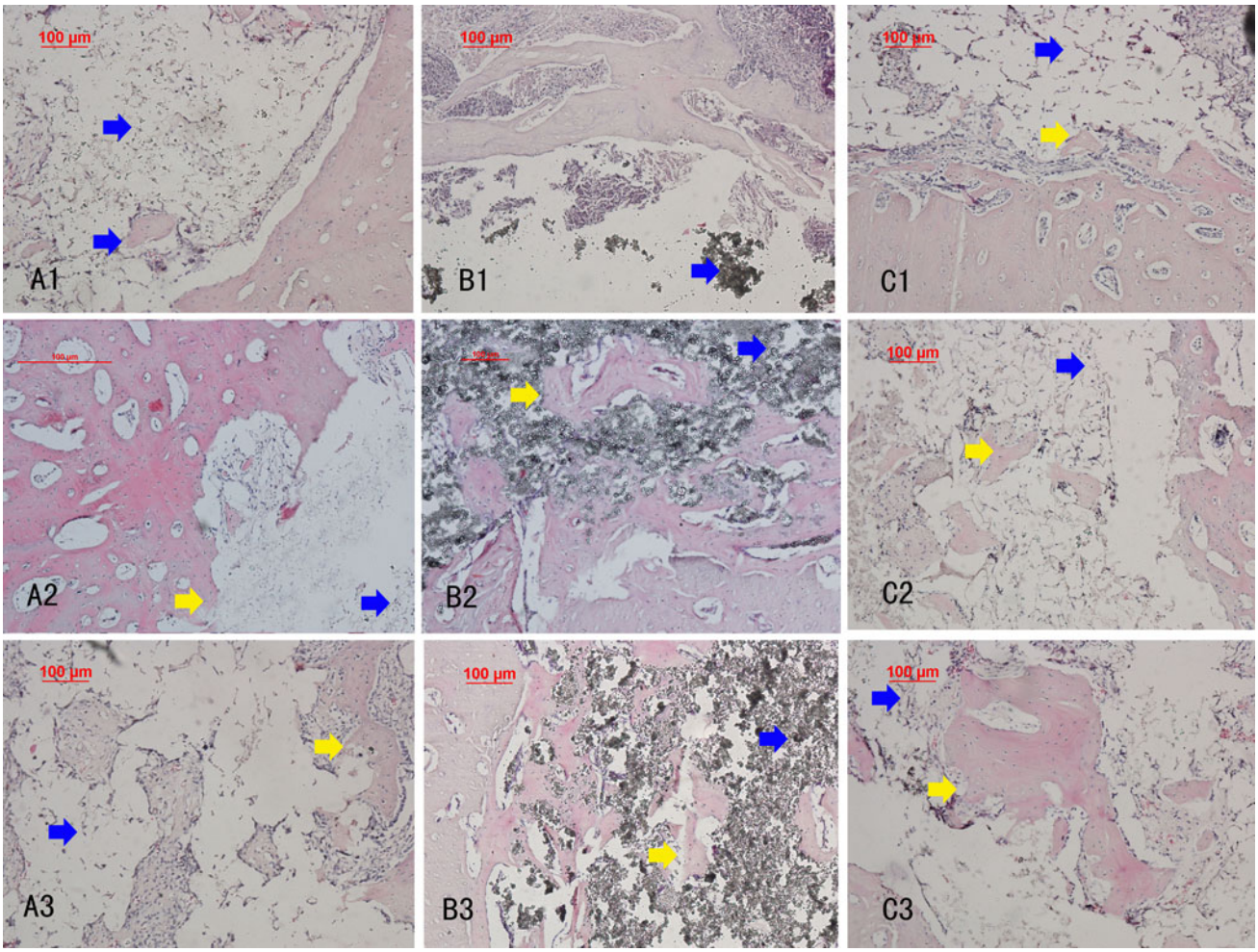

Fig. 8 Histological sections of CPP, HA and K/Sr–CPP scaffolds after 4(**a1**, **b1**, **c1**), 8(**a2**, **b2**, **c2**) and 12(**a3**, **b3**, **c3**) weeks of bone implantation (CPP: **a1**, **a2**, **a3**; HA: **b1**, **b2**, **b3**; K/Sr–CPP: **c1**, **c2**, **c3**). A series of *yellow arrows* pointed the new bone. A series of *blue arrows* pointed the scaffolds (Color figure online)

trabecular structure encasing the scaffold was consistently seen (Fig. 8c3). In the case of the HA group, new bone combine with the HA scaffolds closely and the degradation of HA was only minor or virtually absent in implants during the 12 weeks analysis period (Fig. 8b3).While in the center of the materials, it was observed no new bone or the degradation of HA scaffolds. In the case of the CPP group, host bone formed a close union while the new bone regenerated and penetrated through the interconnective pores to the margin of the scaffolds (Fig. 8a3).

The course of the foreign body reaction (FBR) against scaffolds implants as showed in the histochemical staining on plastic embedded sections (Fig. 8). The degradation of HA was only minor or virtually absent in implants during the 12 weeks analysis period. The degradation of CPP was slow in implants during the 12 weeks analysis period. In contrast, the degradation of K/Sr–CPP had commenced at week 4, although only a few cells had infiltrated. The degradation had advanced at week 8 and was characterized with increased cellular influx surrounding the scaffolds. Within 12 weeks, the majority of K/Sr–CPP been degraded. It was clear that the degradation rate was K/Sr–CPP > CPP > HA during the entire period, while the rate of new bone formed was K/Sr–CPP > HA > CPP during the entire period.

To quantitatively determine the amount of newly formed bone, we statistically analyzed the histological sections of different implantation periods. Figure 9 shows NBV a each implantation period. Obviously, before 8 weeks post-implantation, the amounts of newly formed bone in K/Sr–CPP group increased dramatically, much more than that of CPP scaffold. After that period, however, the rate of bone formation in K/Sr–CPP scaffold slowed down, while in CPP scaffold the speed of new bone formation gradually grew. In HA scaffold group the speed of new bone formation slowly increased during the 12 weeks analysis period. These results demonstrated that K/Sr–CPP scaffolds presented higher efficiency of bone formation than CPP and HA scaffolds at the long term (12 weeks analysis period).

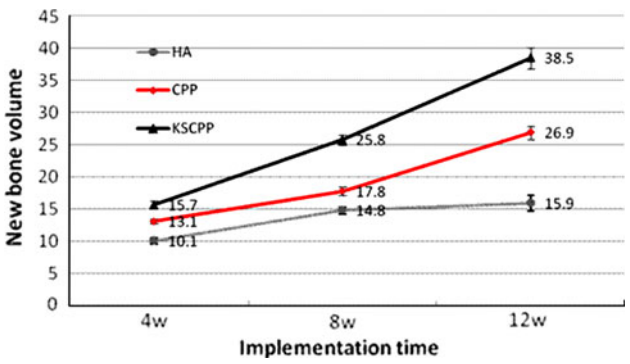

Fig. 9 Quantification of newly formed bone was performed using statistical analysis of histological sections. *Error bars* represent means ± SD for $n = 3$

4 Discussion

Calcium phosphate bioceramics have been widely researched as repairing materials in bone tissue engineering. Ion-substitution is a commonly approach to modify ceramics properties. It was currently applied on bioceramics in bone tissue engineering [24, 25]. Doping method on bioceramics is currently considered to be another approach for improving the biodegradability of CPP. The purpose of this study is to develop a degradable bioceramics by using ion-substituted CPP and aimed to investigate the biocompatibility and osteogenesis of K/Sr–CPP

The general crystalline type of ion-substituted and co-substituted CPP was not changed, the crystallinity varied from different substituted CPP [26]. The substituted CPP was design to serve as bone scaffold guiding the migration, adhesion, and proliferation of osteoblast. The new bone formation induced by scaffold was identified as the extracellular matrix production of differentiated osteoblast adhering on its surface [27]. The Ca–P substrate engulfed by osteoclasts and new Ca–P substrate laid down by osteoblasts. The higher osteoblastic proliferation in substituted CPP was probably also due to the uptake of released doping elements, such as K, and Sr, which are known to be essential in cell activity.

In the present study, Human osteoblast-like cells (MG63) were cultured. The proliferation of cells in direct contact with scaffolds was analyzed with light microscopy and quantitatively with MTT assay. According to the results, we come to the conclusion that K/Sr–CPP scaffold have no negative effect on the attachment and proliferation of MG63, and they are in vitro biocompatible and noncytotoxic to cells.

The results of in vitro experiments prompted us to study the scaffold materials in vivo. So a rabbit model was used to investigate the hard tissue response to HA and K/Sr–CPP scaffold. The rabbit mandible defect was selected as the orthopedic model for this experiment, because it has been proved feasible to assess the performance of biomaterials in bone site. To monitor the process of the formation of bone tissue, histological studies was performed on the specimens after different implantation periods. Active bone regeneration in the mandible defects was found in both HA scaffold and K/Sr–CPP scaffold constructs. In various implantation periods, however, the processes of bone regeneration were different between these two groups. The findings from histology indicate that the K/Sr–CPP scaffold has good biocompatibility and osteoconductivity. Within 12 weeks post-implantation, the contact of bone to the

material was intimate and direct without intervention of soft tissue and new bone density was almost similar to host bone, underlining the complete osteointegration of the defect area.

Osteoinductivity, defined as the ability of the biomaterial to induce new bone tissue formation without the presence of osteogenic factors, is an important property of bone implant materials [28]. Although beta-CPP was regarded as an osteoionductive material which can support bone regeneration [5, 6], however, the ability of inducing ectopic bone formation is not directly mediated by this material.

Osteoconductivity, defined as the ability of the biomaterial scaffold or template to guide the regeneration of new bone tissue along their surfaces, is another important property for bone implant materials [28]. When implanted into body, the osteoconductive property of the bone substituted materials can accelerate and improve the regeneration of new bone tissue. From the bone implant data, it is clearly seen that the addition of K^+ and Sr^{2+} can improve the degradability and osteoconductivity of CPP.

5 Conclusion

In this work, a novel calcium polyphosphate based bioceramics doping with 8 mol% K^+ and 2 mol% Sr^{2+} was prepared by gravity sintering. The in vitro results indicated that the unit cell volume, a–, b– and c–axis unit cell parameters was decreased after K^+ and Sr^{2+} doped into CPP structure. The crystallinity decreased from 86.74% for pure CPP to 70.32% for K/Sr–CPP, while the grain size increased. Besides, the doped ions can significantly improve the degradation behavior and mechanical property. In addition, the proliferation of MG63 revealed that the K/Sr–CPP scaffold exhibits lower cytotoxicity than CPP and HA scaffolds. The in vivo results indicated that the K/Sr–CPP shown a better tissue biocompatibility, biodegradability, osteoinductivity and osteoconductivity. All of these results testified the K/Sr–CPP scaffold was a good candidate for bone implantation.

Acknowledgment The authors would like to acknowledge NSFC Grant No.30870614 for its support to this project. They wish to thank the Centre of Analysis and Testing of Sichuan University for SEM and XRD measurements.

References

1. Pilliar RM, Filiaggi MJ, Wells JD, Grynpas MD, Kandel RA. Porous calcium polyphosphate scaffolds for bone substitute applications—in vitro characterization. Biomaterials. 2001;22:963–72.
2. Grynpas MD, Pilliar RM, Kandel RA, Renlund R, Filiaggi M, Dumitriu M. Porous calcium polyphosphate scaffolds for bone substitute applications in vivo studies. Biomaterials. 2002;23:2063–70.
3. Sayegh TY, Pilliar RM, McCulloch CA. Attachment, spreading, and matrix formation by human gingival fibroblasts on porous–structured titanium alloy and calcium polyphosphate substrates. J Biomed Mater Res A. 2002;61:482–92.
4. Waldman SD, Grynpas MD, Pilliar RM, Kandel RA. Characterization of cartilagenous tissue formed on calcium polyphosphate substrates in vitro. J Biomed Mater Res. 2002;62:323–30.
5. Park EK, Lee YE, Choi JY, Oh SH, Shin HI, Kim KH, et al. Cellular biocompatibility and stimulatory effects of calcium metaphosphate on osteoblastic differentiation of human bone marrow–derived stromal cells. Biomaterials. 2004;25:3403–11.
6. Yang SM, Kim SY, Lee SJ, Ku Y, Han SB, Chung CP. Tissue response of calcium polyphosphate in beagle dog. Part II: 12 Month Result. Key Eng Mater. 2004;218:657–60.
7. Ding YL, Chen YW, Qin YJ, Shi GQ, Yu XX, Wan CX. Effect of polymerization degree of calcium polyphosphate on its microstructure and in vitro degradation performance. J Mater Sci Mater Med. 2008;19:1291–5.
8. Gomez F, Vast P, Llewellyn P, Rouquerol F. Dehydroxylation mechanisms of polyphosphate glasses in relation to temperature and pressure. J Non–Cryst Solids. 1997;222:415–21.
9. Dias AG, Lopes MA, Gibson IR, Santos JD. In vitro degradation studies of calcium phosphate glass ceramics prepared by controlled crystallization. J Non–Cryst Solids. 2003;330:81–9.
10. Song W, Tian M, Chen F, Tian Y, Wan C, Yu X. The study on the degradation and mineralization mechanism of ion–doped calcium polyphosphate in vitro. J Biomed Mater Res B. 2008;89:430–8.
11. Wang Q, Song W, Wang Q, Zhang X, Yu X, Wan C. The research on degradability, mineralization and mechanical properties of co–substituted calcium polyphosphate as a new kind of bone repair material. J Funct Mater. 2009;40:1506–9.
12. Qiu K, Wan C, Zhao C, Chen X, Tang C, Chen Y. Fabrication and characterization of porous calcium polyphosphate scaffolds. J Mater Sci. 2006;41:2429–34.
13. Wurst J, Nelson J. Lineal Intercept Technique for Measuring Grain Size in Two Phase Polycrystalline Ceramics. J Am Ceram Soc. 1972;55:109.
14. Fiske C, Subbarow Y. The colorimetric determination of phosphorus. J Biol Chem. 1925;66:37.
15. Dion A, Langman M, Hall G, Filiaggi M. Vancomycin release behaviour from amorphous calcium polyphosphate matrices intended for osteomyelitis treatment. Biomaterials. 2005;26:7276–85.
16. Nalçacı A, Öztan MD, Yılmaz Ş. Cytotoxicity of composite resins polymerized with different curing methods. Int Endod J. 2004;37:151–6.
17. Qiu K, Wan C, Chen X, Zhang Q, Su H. In vitro degradation studies of calcium polyphosphate ceramics prepared by controlled degree of polymerization and crystallization. Adv Biomater VI. 2005;288–289:553–6.
18. Wang Q, Wang J, Zhang X, et al. Degradation kinetics of calcium polyphosphate bioceramic: an experimental and theoretical study. Mater Res. 2009;12:495–501.
19. Hutmacher DW. Scaffolds in tissue engineering bone and cartilage. Biomaterials. 2000;21:2529–43.
20. Zhou L. Tutorial of physical chemistry. 1st ed. Beijin: Science publishing company; 2002.
21. Chen Y, Shi G, Ding Y, Yu X, Zhang X, Zhao C, et al. In vitro study on the influence of strontium–doped calcium polyphosphate on the angiogenesis –related behaviors of HUVECs. J Mater Sci Mater Med. 2008;19:2655–62.

22. Tian M, Chen F, Song W, Song Y, Chen Y, Wan C, et al. In vivo study of porous strontium–doped calcium polyphosphate scaffolds for bone substitute applications. J Mater Sci Mater Med. 2009;20:1505–12.
23. Qiu K, Zhao X, Wan C, Zhao C, Chen Y. Effect of strontium ions on the growth of ROS17/2.8 cells on porous calcium polyphosphate scaffolds. Biomaterials. 2006;27:1277–86.
24. Kim SR, Lee JH, Kim YT, Riu DH, Jung SJ, Lee YJ, Chung SC, Kim YH. Synthesis of Si, Mg substituted hydroxyapatites and their sintering behaviors. Biomaterials. 2003;24:1389–98.
25. Webster TJ, Massa–Schlueter EA, Smith JL, Slamovich EB. Osteoblast response to hydroxyapatite doped with divalent and trivalent cations. Biomaterials. 2004;25:2111–21.
26. Song W, Wang Q, Wan C, Shi T, Markel D, Blaiser R, et al. A novel alkali metals/strontium co–substituted calcium polyphosphate. J Biomed Mater Res Part B: Appl Biomater. 2011;98B:255–62.
27. LeGeros RZ. Calcium Phosphate Based Osteoinductive Materials. Chem Rev. 2008;108:4742–53.
28. Albrektsson T, Johansson C. Osteoinduction, osteoconduction and osseointegration. Eur Spine J. 2001;10:S96–101.